Optimizing Hydrogen-Bonding in Creating Miscible Liquid Crystalline Polymer Blends by Structural Modification of the Blend Components

Sriram Viswanathan and M. D. Dadmun*

Department of Chemistry, The University of Tennessee at Knoxville, Knoxville, Tennessee 37996

Received September 23, 2002

ABSTRACT: Our recent experimental results have shown that a miscible blend containing a liquid crystalline polymer (LCP) and an amorphous copolymer, both capable of self-association and interassociation by hydrogen-bonding, can be created by slight structural modification of the amorphous polymer. The results also show that an optimum amount of intermolecular H-bonding can be formed in the blend by systematically varying the distance between the hydrogen-bonding groups on the copolymer chain. It was found that the system with the optimum amount of intermolecular hydrogen-bonding is also the system with the broadest miscibility window. In this paper, this work is extended by examining the effect of elimination of self-associating hydrogen bonds in the LCP on the intermolecular hydrogen-bonding and on the phase behavior of these blends. FTIR and phase behavior results show that this modification results in increased intermolecular hydrogen-bonding and a broader miscibility window than the blend that contains the original liquid crystalline polymer. In agreement with our previous results, the optimum amount of intermolecular H-bonding is formed in the blend by systematically varying the distance between the hydrogen-bonding groups on the amorphous copolymer. DSC and optical microscopy correlate these data to the blend phase behavior to show that the optimum amount of intermolecular hydrogen-bonding correlates to the system with the broadest miscibility window. Finally, thermodynamic analysis of these blends provides insight and guidelines regarding the applicability of this scheme to create a miscibility window in other polymer blends.

Introduction

Recent scientific research and development of polymers has often concentrated on understanding, developing, and controlling multicomponent polymer systems, including blends. The motivation for this work is often reduced product cost, tailored properties, and improved processability.[1−10] Liquid crystalline polymers (LCP) have many desirable properties including significant orientation in flow, which correlates to excellent tensile properties in the solid state and lower viscosity and thus improved processability. Although LCP have found significant use in high-strength fibers and plastics,[11−15] their high cost has limited their use in broad commercial applications.[16−22] One solution to this limitation may be to blend rigid LCP with flexible, commodity amorphous polymers. The resultant rod/coil polymer composites would be cost-effective and possess enhanced mechanical properties and processability. Unfortunately, the task of mixing two polymers to create a new material is not trivial due to their small entropy of mixing combined with the significant contribution of an unfavorable enthalpy of mixing to the Gibbs free energy of the process. The end result is often a phase-separated blend with weak interfaces and poor blend properties.[23−25]

While structural dissimilarity of chains does not always play a significant role in a blend where the polymer chains are flexible, it becomes an important factor in rod−coil polymer blends. Structural dissimilarity between rigid and flexible polymers tends to segregate the rigid polymer chains into an anisotropic phase where they align themselves, separating out from the isotropic phase, which consists mostly of the flexible polymers.[26]

To facilitate the creation of molecular composites consisting of rod and coil polymers, it is often important to form strong, specific interactions between the two polymers. Flory−Huggins theory holds the assumption that the polymer chains mix randomly in a blend,[26,27] but this assumption finds its limitation in the presence of strong, specific interactions such as hydrogen-bonding since the polymer chains are forced into nonrandom configurations by these interactions. Painter et al. have developed an association model[5,6,28,29] that adds a free energy term (ΔG_H) to the Flory−Huggins theoretical expression to account for these changes in enthalpy and entropy due to hydrogen-bonding interactions.

$$\frac{\Delta G_m}{RT} = \frac{\Phi_A}{M_A} \ln \Phi_A + \frac{\Phi_B}{M_B} \ln \Phi_B + \chi_{AB}\Phi_A\Phi_B + \frac{\Delta G_H}{RT}$$

This model employs a suitable equilibrium constant to account for the dynamic equilibrium of the breaking and re-forming of hydrogen bonds.

The extent of intermolecular H-bonding (H-bonding between dissimilar polymer chains) is an important parameter in determining the miscibility of a blend with specific interactions. Although strong, specific interactions can produce a favorable enthalpy of mixing in the blend, it is to be noted that such interactions tend to further minimize the entropy of the system due to limitations on the chain mobility and its rotational freedom as the polymer chains are forced to assume nonrandom configurations. Thus, the effect of specific interactions on the free energy of mixing two polymers is complex and must be thoroughly understood to enable the prediction of guidelines to utilize them to induce miscibility in blends.

In addition to intramolecular H-bonding, functional group accessibility impacts the formation of intermolecular hydrogen bonds. Steric shielding of functional groups due to the presence of bulky side chain groups, steric crowding of hydrogen-bonding groups due to

10.1021/ma021520c CCC: $25.00
Published on Web 04/10/2003

limited spacing between the groups on a polymer chain, and intramolecular screening due to flexible chains bending back upon themselves are some of the important factors that must be considered.[30−37]

Studies by Landry et al.[8,42,43] reveal that the driving force for miscibility in blends of poly(vinylphenol) (PVPh) and poly(styrene-*co*-4-vinylphenol) (PS-*co*-VPh) with polymers such as polyesters, polyurethanes, and polyamides is intermolecular hydrogen-bonding between the phenolic hydroxyl and carbonyl groups. They have confirmed the significance of the role of hydrogen-bonding in the miscibility of blends involving PVPh by providing correlation between the blends thermal behavior and the amount of intermolecular hydrogen-bonding. Additionally, Painter et al.[18,40] and Green et al.[41] have demonstrated that miscibility in LCP/amorphous polymer blends can be attained by the presence of intermolecular hydrogen-bonding between the two polymers. However, a detailed, systematic study to provide guidelines to apply these results to a broad range of systems has not been presented.

In our earlier work,[38,39] we examined mixtures containing a liquid crystalline polyurethane (LCPU) and an amorphous copolymer, poly(styrene-*co*-4-vinylphenol) (PS-*co*-VPh).[38,39] FTIR demonstrates that the extent of intermolecular H-bonding between the LCP and the amorphous copolymer can be optimized by systematically varying the PS-*co*-VPh copolymer composition. This variation controls the distance between the hydroxyl groups along the PS-*co*-VPh chain, which in turn impacts the extent of intermolecular hydrogen-bonding. Moreover, phase behavior studies demonstrate that the copolymer that exhibits the optimum amount of intermolecular hydrogen-bonding also has the broadest miscible window in the phase diagram.

In this work, we extend that previous study to examine the impact of altering the *intramolecular* hydrogen-bonding ability of the liquid crystalline polymer on the intermolecular hydrogen-bonding and phase behavior of the blends. To be more specific, the liquid crystalline polyurethane is methylated to remove the amide hydrogen, thus forming the *N*-methyl liquid crystalline polyurethane (LCPU-M). This step eliminates the possibility of C═O···H−N hydrogen-bonding among the LCP chains, which should increase the number of C═O groups in the LCP available for intermolecular H-bonding with the hydroxyl groups of the PS-*co*-VPh. This paper will therefore present FT-IR and phase behavior data of LCPU-M/PS-*co*-VPh blends and compare them to the results obtained for LCPU/PS-*co*-VPh blends to illustrate the effect of eliminating intramolecular H-bonding in LCP chains on the amount of intermolecular H-bonding in the blend and on the blend phase behavior.

Experimental Section

Materials. 4,4-Biphenol and 2,4-toluene diisocyanate (TDI) were obtained from TCI America Inc., styrene, 4-acetoxystyrene, and hydrazine hydrate were purchased from Aldrich Chemical Co., azobis(isobutyronitrile) (AIBN) was purchased from Dojac Inc., and sodium hydroxide, 6-chlorohexanol, methanol, dioxane, *N,N′*-dimethylformamide (DMF), and 1-butanol were purchased from Fisher-Acros. Poly(4-vinylphenol) (PVPh) was purchased from Polysciences Inc. In the polymerization of the liquid crystalline polyurethane (LCPU), DMF, 1-butanol, and TDI were purified by vacuum distillation before use. All other chemicals were used as received. For the synthesis of the LCPU-M, sodium hydride and methyl iodide were purchased from Aldrich Chemical Co. and *N,N*-dimethylformamide (DMF) and methanol from Fisher-Acros Co. DMF was purified by vacuum distillation before use.

Polymer Synthesis. Synthesis of the Liquid Crystalline Polyurethane (LCPU). The liquid crystalline polyurethane was synthesized by the condensation of 4,4′-bis(6-hydroxyhexoxy)biphenyl (BHHBP) and 2,4-toluene diisocyanate (2,4-TDI).[44] The procedure for the synthesis of the liquid crystalline polyurethane is identical to our previous work.[38,39]

Synthesis and Characterization of LCPU-M. The *N*-methyl liquid crystalline polyurethane (LCPU-M) was prepared by reacting the LCPU with sodium hydride and methyl iodide using the method of Mihara and Koide[45] as described below. In an atmosphere of nitrogen, sodium hydride (0.053 g, 0.0022 mol) suspended in 2 mL of DMF was stirred in a chilled reaction vessel. A DMF solution of LCPU (0.4 g, 0.000 66 mol) was added to the suspension of sodium hydride. After the reaction mixture was stirred for 30 min, methyl iodide (0.2 mL, 0.0032 mol) was added dropwise to the mixture. Following stirring of the reaction mixture for 2 h, excess sodium hydride was removed by filtration. The filtrate was concentrated and poured into a large amount of methanol, and the obtained precipitate was washed with methanol (yield 75%). FT-IR (not presented here) and proton NMR characterization of the LCPU-M both verify the complete conversion of LCPU to LCPU-M. ^{1}H NMR (see Figures 1 and 2) (reported as chemical shift, multiplicity, integration, assignment) [δ 7.47 (m, 5H, a), 6.96 (m, 6H, b), 3.96 (m, 8H, c), 3.4 (s, 6H, d), 2.09 (s, 3H, e), 1.65 (m, 8H, f), 1.40 (m, 8H, g)].

Synthesis of Poly(styrene-*co*-4-vinylphenol) Copolymers. Poly(styrene-*co*-4-vinylphenol) (PS-*co*-VPh) random copolymers were prepared by the free radical polymerization of styrene and 4-acetoxystyrene using AIBN as the initiator followed by the hydrolysis of the acetoxy groups using hydrazine hydrate according to the procedure of Green and Khatri.[41] Copolymers containing 5, 10, 20, 30, 40, and 50 mol % vinylphenol were synthesized and utilized in this study. Hereinafter, PS-*co*-VPh(*n*) denotes a PS-*co*-VPh copolymer with *n* mol % VPh. As an example, the procedure for the synthesis of PS-*co*-VPh(10) is shown below.

First, styrene (2.7 mL, 23.56 mmol), 4-acetoxystyrene (0.4 mL, 2.62 mmol), and AIBN (0.0104 g) were transferred into a three-neck round-bottom flask filled with dioxane (50 mL) under a mild flow of argon. The flask equipped with a water-jacketed condenser was heated at 60°C for 18 h. The solution was then poured into methanol to precipitate the poly(styrene-*co*-4-acetoxystyrene) as the product. The polymer was dried in a vacuum oven for a day (yield 82%). ^{1}H NMR peak assignments: 1.4 ppm (2H, d, CH_2); 1.7 ppm (1H, t, CH); 2.2 ppm (3H, s, $-OCOCH_3$); 6.2−7.2 ppm (9H, m, aromatic H).

Next, the hydrolysis of acetoxy groups to hydroxyl groups was carried out by the dissolution of 2 g of poly(styrene-*co*-4-acetoxystyrene) in dioxane (40 mL) in a round-bottom flask.[46] Hydrazine hydrate (6 mL) was then added to this solution and stirred for 40 h at room temperature. The polymer was precipitated into methanol and dried in a vacuum oven for 24 h. The completion of hydrolysis was verified by the disappearance of the methyl peak of acetoxy group at 2.2 ppm in the NMR spectrum. The procedure for determination of the composition of the PS-*co*-VPh are identical to those discussed in our previous publication.[39] Table 1 lists the molecular weight characteristics and thermal behavior of the liquid crystalline polymers and the amorphous copolymers.

Polymer Characterization. The synthesized polymers were analyzed for their molecular weights using a Waters gel permeation chromatograph equipped with Ultrastyragel columns with a refractive index detector. DMF was used as elution solvent for the LCPU and the LCPU-M and tetrahydrofuran for PS-*co*-VPh copolymers. Polystyrene with a narrow molecular weight distribution was used as calibration standard for all polymers. Thermal behavior of the polymers and blends was analyzed using differential scanning calorimetry, and measurements were made at 10 °C/min using a Mettler DSC 821 calibrated with indium. Proton NMR spectroscopy (250 MHz Bruker) with TMS as the internal standard was used to

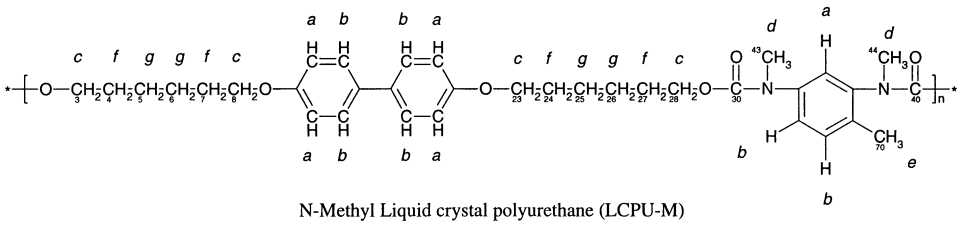

N-Methyl Liquid crystal polyurethane (LCPU-M)

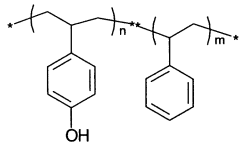

Poly(Styrene-co-4-vinyl phenol)

Figure 1. Structures of the liquid crystalline polyurethane (LCPU), *N*-methyl liquid crystalline polyurethane (LCPU-M), and poly(styrene-*co*-4-vinylphenol) (PS-*co*-VPh) copolymers used in this study. Lower case italic letters refer to proton NMR results (see also Figure 2).

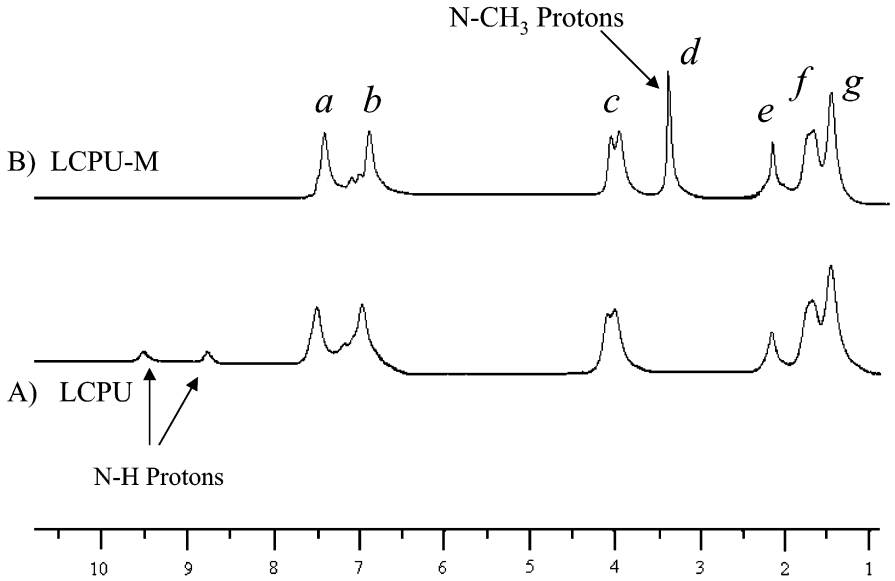

Figure 2. Proton NMR spectra of LCPU (curve a) and LCPU-M (curve b). Lower case italic letters refer to protons from specific groups (see also Figure 1).

Table 1. Molecular Weights and Phase Transitions of Pure LCPU, LCPU-M, and PS-*co*-VPh Copolymers

	mol wt (g/mol)		phase transition temperature[a] (°C)		
polymer	M_n	M_w	T_g	T_m	T_i
pure LCPU	35 000	53 600	87	132	160
pure LCPU-M	37 000	56 700	72	117	134
PS-*co*-VPh(5)	13 700	21 300	101		
PS-*co*-VPh(10)	20 700	34 500	103		
PS-*co*-VPh(20)	47 100	90 100	105		
PS-*co*-VPh(30)	22 100	32 400	108		
PS-*co*-VPh(40)	31 300	61 100	114		
PS-*co*-VPh(50)	34 100	65 200	116		
pure PVPh	22 000		147		

[a] T_m = crystalline melt temperature; T_i = nematic-to-isotropic transition temperature.

determine the composition of the LCPU, LCPU-M, and PS-*co*-VPh copolymers. The solvents used for the NMR experiments were deuterated dimethyl sulfoxide for the LCPU and LCPU-M and deuterated chloroform for the PS-*co*-VPh copolymers.

IR spectra were obtained on a Biorad FTS-60A Fourier transform infrared (FT-IR) spectrometer purged with dried air using a minimum of 64 scans at a resolution of 2 cm^{-1}. The frequency scale was internally calibrated with a He−Ne reference to an accuracy of 0.2 cm^{-1} and externally with polystyrene. Solvent casting of LCPU/PS-*co*-VPh and LCPU-M/PS-*co*-VPh blends from 2% (w/v) DMF solutions on KBr disks at room temperature created samples for FT-IR studies. The KBr disks were placed on a horizontal holder in a desiccator to reduce the evaporation rate and to avoid film cracking. After evaporating most of the solvent at room temperature, the disks were subsequently dried in a vacuum oven at 60 °C for 3 days to remove residual solvent and moisture. The absence of solvent in the sample was verified by the absence of the C═O peak of DMF, which occurs at 1650 cm^{-1} in the IR curve, a lower wavenumber than the C═O peak of the LCPU-M (1705 cm^{-1}). The films prepared for FTIR were adequately thin to be within an absorbance range where the Beer−Lambert law is satisfied. High-temperature spectra were obtained using a cell mounted in the spectrometer connected to a temperature controller. The temperature was controlled to an accuracy of 0.5 °C. Phase behavior data of the blends were obtained by preparing 2% (w/v) solutions of the blend in DMF and spotting them on a microscope slide. The solvent was allowed to evaporate in a desiccator first and then overnight in a vacuum oven at 60 °C to remove residual

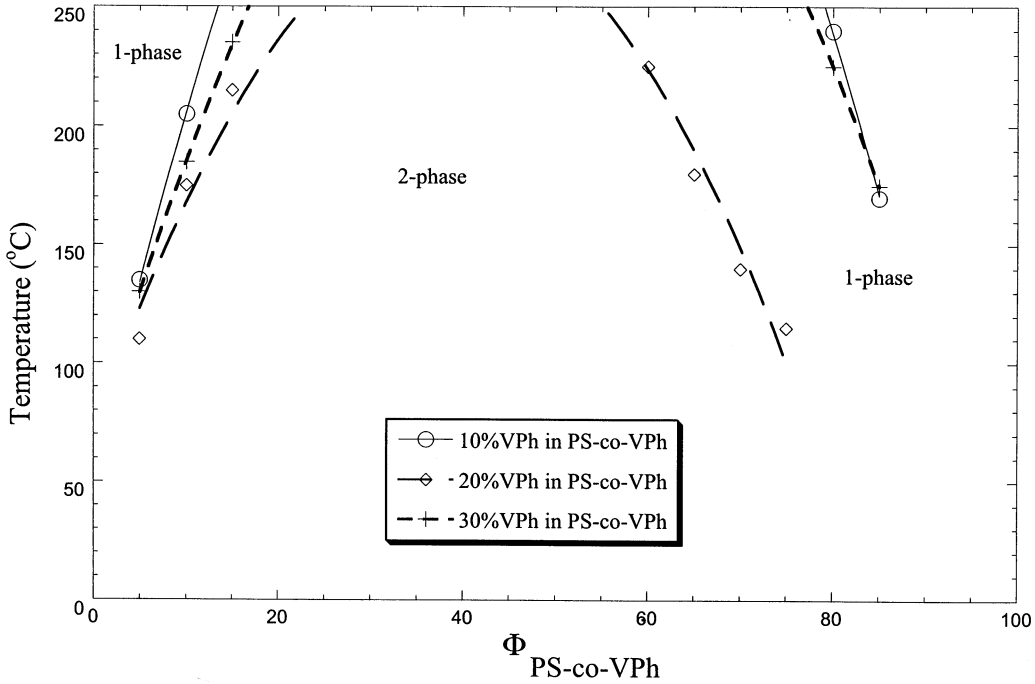

Figure 3. Phase diagram of blends containing LCPU and PS-*co*-VPh as determined from phase contrast optical microscopy.[39] The lines are meant to guide the eye.

solvent. The phase behavior of the blends was also monitored by phase contrast and polarized optical microscopy using an Olympus BH-2 optical microscope equipped with a Mettler FP82HT hot stage.

Results

Our recent results[38,39] demonstrate that a true molecular composite can be created by optimizing the extent of intermolecular interactions between a liquid crystalline polyurethane and an amorphous copolymer. In that study, altering the composition of an amorphous copolymer systematically varies the extent of intermolecular hydrogen-bonding between the two components, where the amorphous copolymer contains one monomer (vinylphenol) that can participate in hydrogen-bonding while the other monomer cannot (styrene). The results, shown in Figure 3,[39] demonstrate that increased spacing of the hydroxyl groups along the copolymer chain provides the necessary rotational freedom to allow the functional groups to find and properly orient relative to the carboxyl group of the LCP. Of course, if the hydroxyl groups are too dilute, insufficient interacting moieties exist, and the amount of intermolecular bonds is limited. Thus, the formation of an optimum amount of *intermolecular* hydrogen bonds occurs where these two contributions (rotational freedom vs dilution) are balanced. In the work described here, we seek to extend this finding to provide further parameters that may be manipulated to improve the miscibility in such systems. Therefore, the aim of this study is to understand the correlation between the liquid crystalline polymer structure, the copolymer composition, and the extent of intermolecular H-bonding in a blend containing a LCP and an amorphous copolymer and then correlate this information to the phase behavior of that blend.

In LCPU/PS-*co*-VPh blends,[38,39] the extent of intermolecular hydrogen-bonding between the two polymer components is quantitatively determined using FT-IR. Likewise, in LCPU-M/PS-*co*-VPh blends, the same procedure of curve fitting is used (using Peakfit software version 3.0) the carbonyl stretching vibration (around 1700 cm^{-1}) of the FT-IR curve has been analyzed to determine the percentage of carbonyl groups in the system participating in intermolecular H-bonding between the two blend components. The IR curves of the blends were examined at a series of temperatures ranging from room temperature to 180 °C. While there is very little difference in the trends described in this paper with temperature, the data at 180 °C (above the T_g and T_m of the blend components) are reported to ensure that ordering of the LCP does not influence the results. Also, it is well-known that blends that are formed by solvent casting often do not represent equilibrium structures due to varying polymer−solvent interactions among the blend constituents. By analyzing data at 180 °C, the samples were allowed to reach equilibrium conditions, in contrast to the nonequilibrium condition that would exist in as-cast samples. In the LCPU-M blends, contributions to this C═O stretching envelope are assigned to free (non-hydrogen-bonded) C═O groups (around 1705 cm^{-1}) and intermolecularly H-bonded C═O groups (to O−H groups) (around 1680 cm^{-1}).

As mentioned in our previous work, the percentage of O−H groups on the copolymer that is intermolecularly H-bonded to the C═O cannot be determined quantitatively by curve fitting the O−H stretching band at 3300 cm^{-1}. This is primarily due to the difficulty of quantitative analysis of the hydroxyl region due to vibration overlap of all the contributing peaks, thus giving rise to a very broad O−H peak.[47] Also, this O−H peak is plagued by the presence of the overtone of the fundamental C═O stretching vibration.[48] Therefore, the amount of O−H groups that is involved in intermolecular H-bonding is estimated stoichiometrically. The percent of O−H groups that participate in intermolecular H-bonding is estimated by dividing the experimentally determined percent of C═O groups participating in hydrogen-bonding by the ratio of the number of O−H

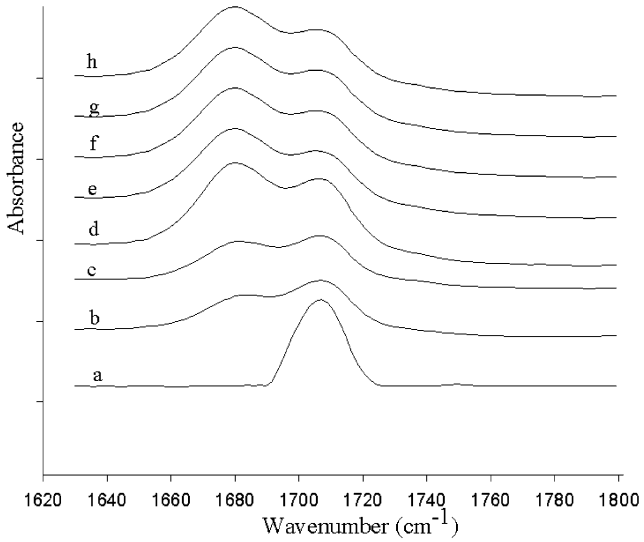

Figure 4. FT-IR spectra of C═O stretching region for blends containing 80 wt % PS-*co*-VPh and 20 wt % LCPU-M measured at 180 °C. Curve (a) is the pure LCPU-M, while the remaining curves are for blends containing PS-*co*-VPh with (b) 5, (c) 10, (d) 20, (e) 30, (f) 40, (g) 50, and (h) 100 mol % VPh.

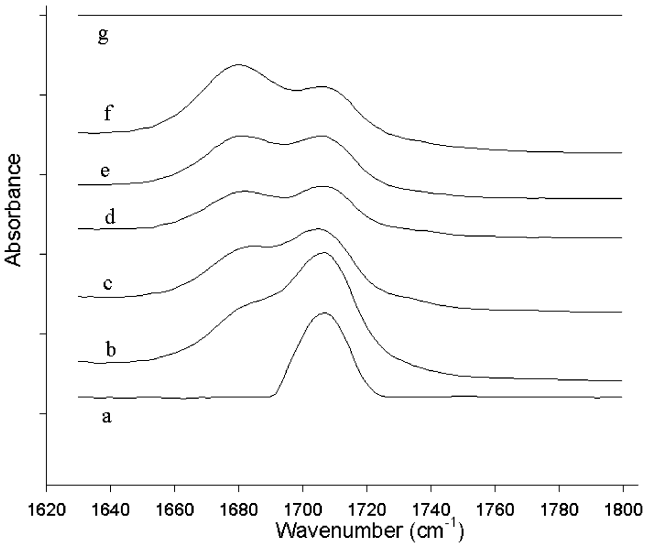

Figure 5. FT-IR spectra of the C═O stretching region for blends containing LCPU-M and PS-*co*-VPh(40) measured at 180 °C. The curves correspond to blends with a composition of (LCPU-M/PS-*co*-VPh wt/wt): (a) 100/0, (b) 80/20, (c) 60/40, (d) 50/50, (e) 40/60, (f) 20/80, and (g) 0/100.

groups to C═O groups present in the blend.[39] Figure 4 shows the FT-IR curves in the C═O stretching region (1800−1650 cm^{-1}) for the blend containing LCPU-M and PS-*co*-VPh (80 wt % PS-*co*-VPh) for various copolymer compositions measured at 180 °C. This figure qualitatively demonstrates the increase in the amount of intermolecular H-bonding with increase in the amount of VPh in the copolymer from 0 to 40% (curves b−f), observed from the increase in the C═O peak at 1680 cm^{-1}. However, there is no significant change observed in this peak above 40% VPh in the copolymer (curves f−h). While Figure 4 provides information on the effect of copolymer composition on the extent of intermolecular hydrogen-bonding for a single composition, the data in Figure 5 show the impact of altering the blend composition on the intermolecular hydrogen-bonding. FT-IR curves of the C═O stretching region of blends that contain LCPU-M and PS-*co*-VPh(40) of various blend compositions measured at 180 °C are shown in Figure 5. This figure shows an increase in the extent of intermolecular H-bonded C═O groups with an increase in the amount of PS-*co*-VPh(40) in the blend from 0 to 80 wt %, which is clearly illustrated by an increase in the peak at around 1680 cm^{-1}.

A more thorough understanding of these curves can be obtained by quantitative determination of the amount of intermolecular H-bonding in these blends by curve fitting the C═O stretching peaks of these IR curves. The area under the two peaks that contribute to the C═O stretching vibration is determined from the curve-fitting procedure; A_1 is the area of the free carbonyl peak, and A_2 is the area of the peak associated with the intermolecularly hydrogen-bonded carbonyls. However, these data cannot simply be used to determine the percentage of carbonyl groups that are intermolecularly hydrogen-bonded, as it is well-known that the absorption coefficient of the hydrogen-bonded band is greater than that of the free band. To account for this difference in absorption coefficients, a ratio of the absorption coefficients of these bands is required. The absorption coefficient ratio (K) was found using the method of Coleman and Painter[6,47,49] to account for these differing absorptivity coefficients.

$$K = [A_{HB}{}^{T_2} - A_{HB}{}^{T_1}]/[A_F{}^{T_1} - A_F{}^{T_2}]$$

where $A_{HB}{}^{T_1}$ and $A_{HB}{}^{T_2}$ are hydrogen-bonded carbonyl absorption intensities at temperatures T_1 and T_2 and $A_F{}^{T_1}$ and $A_F{}^{T_2}$ are free C═O absorption intensities at temperatures T_1 and T_2. The absorption intensity of the hydrogen-bonded C═O band (A_2) was then corrected for the difference in absorptivity coefficients by dividing this area by K ($A_2' = A_2/K$) to determine the percent of C═O groups involved in intermolecular H-bonding, calculated by

$$\% \text{ C═O} = A_2'/(A_1 + A_2')$$

The curve-fitting results for LCPU-M/PS-*co*-VPh blends containing 80 wt % PS-*co*-VPh for various copolymer compositions measured at 180 °C are listed in Table 2.

Figure 6 is a plot of the percent of C═O that are intermolecularly hydrogen-bonded to O−H as a function of mole percent VPh in the copolymer for various blend compositions of LCPU-M/PS-*co*-VPh blends measured at 180 °C. In the LCPU-M blends, the amount of C═O that participates in intermolecular H-bonding increases up to 40 mol % VPh but levels off above 40%. The logical interpretation of this curve is that as the amount of VPh increases from 0 to 40%, more hydroxyl groups are introduced that can H bond with C═O groups, and thus the curve increases. However, above 40% VPh in the copolymer, there is very little increase in the amount of intermolecular H-bonding, suggesting that additional O−H groups are unable to find suitably oriented or positioned C═O groups with which to form an intermolecular H bond. When compared to our previously reported results,[39] the LCPU-M blends show an increased percent of C═O intermolecular H-bonding than equivalent LCPU blends for all copolymer compositions studied, signifying a larger number of C═O groups available in the LCPU-M blends for intermolecular H-bonding.

Figure 7 shows the percent of O−H intermolecularly hydrogen-bonded to C═O as a function of mole percent VPh in the copolymer for various blend compositions

Table 2. Curve-Fitting Results of the C═O Stretching Region for Pure LCPU-M and Blends Containing 80 wt % PS-*co*-VPh Copolymer for Various Copolymer Compositions[a]

% VPh in PS-*co*-VPh	free C═O			intermolecularly H-bonded C═O			% C═O intermolecularly H-bonded
	v^b (cm^{-1})	$W_{1/2}$ (cm^{-1})	A_1	v (cm^{-1})	$W_{1/2}$ (cm^{-1})	A_2	
pure LCPU-M	1707	18.0	8.214				
5	1707	18.1	5.750	1682.2	30.2	2.314	20.72
10	1707	18.1	4.473	1680.3	30.6	3.950	36.45
20	1707	18.2	4.075	1679.5	30.5	5.362	46.08
30	1707	18.0	3.262	1679.0	30.8	6.279	55.56
40	1707	18.0	3.084	1678.8	31.0	6.757	58.73
50	1707	18.2	2.924	1678.8	31.0	6.403	58.71
100	1707	18.2	2.833	1678.8	31.0	6.410	59.51

[a] Absorptivity coefficient (K) = 1.54; $A_2' = A_2/K$; $A_T = A_1 + A_2'$. % C═O intermolecularly H-bonded = $(A_2'/A_T) \times 100$. [b] Fixed during curve fitting.

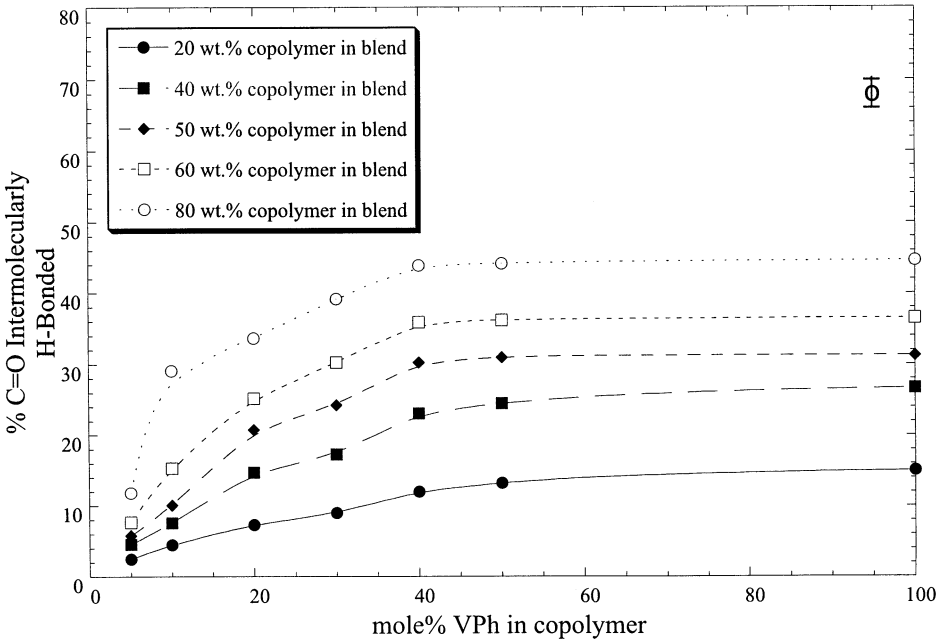

Figure 6. Percent of carbonyl groups participating in intermolecularly hydrogen-bonding as a function of PS-*co*-VPh copolymer composition in blends of LCPU-M and PS-*co*-VPh measured at 180 °C for different blend compositions.

measured at 180 °C. The percentage of O−H that participate in intermolecular hydrogen-bonding does not change much up to 40 mol % VPh in the copolymer but decreases as more O−H groups are included on the copolymer chain. As with the carbonyl study, there is more % O−H intermolecularly hydrogen-bonded in the LCPU-M blends than in equivalent LCPU blends[39] for all copolymer compositions, presumably due to the larger number of C═O groups that are available for intermolecular hydrogen-bonding in LCPU-M blends due to the lack of intramolecular hydrogen bonds in the LCPU-M.

Thus, FT-IR results show that the spacing between O−H groups of the copolymer chains in LCPU-M blends affect the extent of intermolecular H-bonding similar to those in LCPU blends. The results of this "spacing effect" study are in agreement with similar work by Coleman et al.[30] and Radmard et al.,[34] which indicate that the extent of intermolecular H-bonding is an optimum when the hydroxyl groups are distanced apart on the copolymer chain. This increased spacing provide an improvement in the rotational freedom of the functional groups and causes a decrease in the chance of H-bonding between O−H groups, thereby improving the accessibility and availability of O−H for intermolecular hydrogen-bonding with C═O. However, this trend ceases below a critical amount of hydrogen-bonding moiety in the copolymer (40 and 20 mol % in LCPU-M and LCPU blends, respectively), below which the number of hydroxyl groups in the copolymer becomes so low that it limits the number of possible intermolecular H-bonds that can be formed.

To correlate the extent of intermolecular hydrogen-bonding to the phase behavior of these blends, the phase diagrams of blends containing LCPU-M and PS-*co*-VPh that consist of 5%, 10%, 20%, 30%, 40%, and 50% VPh [PS-*co*-VPh(5), PS-*co*-VPh(10), PS-*co*-VPh(20), PS-*co*-VPh(30), PS-*co*-VPh(40), and PS-*co*-VPh(50)] were determined using DSC and optical microscopy. Figure 8 shows the DSC curves of LCPU-M/PS-*co*-VPh(30) blends for various blend compositions. A single glass transition temperature is observed for blend compositions above ca. 55 wt % LCPU that changes with concentration, which suggests miscibility in this regime. Similar curves are found for the other blends, though with differing concentration trends. Figure 9 is a plot of the experimentally determined T_g and the expected T_g of miscible blends as calculated from the Fox−Flory equation for blends containing LCPU-M and PS-*co*-VPh(30). This plot shows that the experimentally determined T_g and the theoretical T_g agree very well for blends with low LCP loading. The experimental and theoretical T_g's begin to deviate above a critical LCP content level. This critical concentration of LCP is approximately 15% LCP

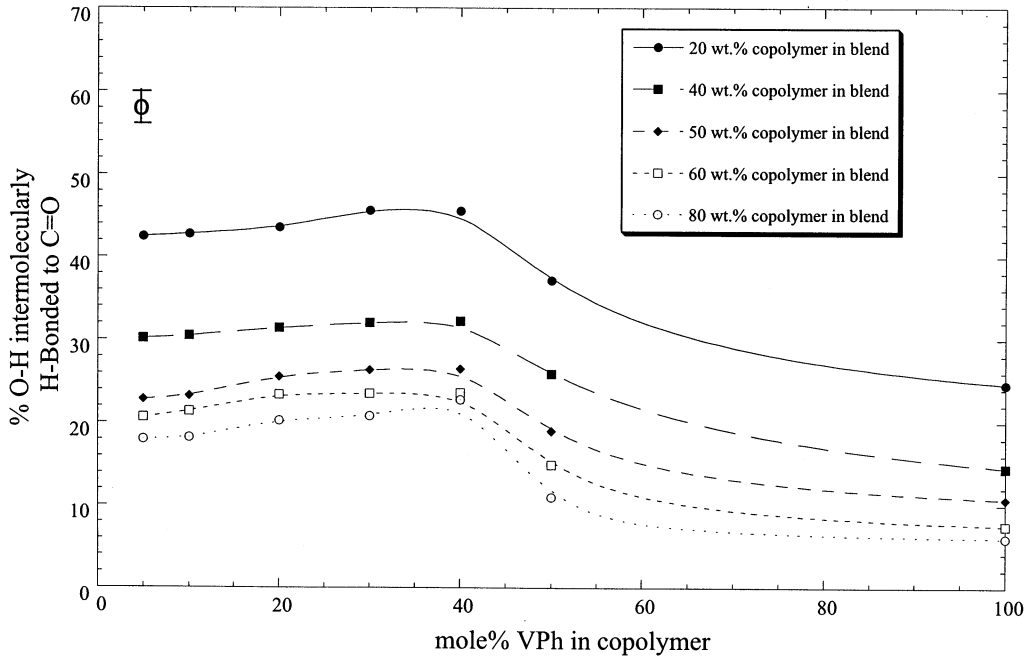

Figure 7. Percent of hydroxyl groups participating in intermolecularly hydrogen-bonding as a function of PS-*co*-VPh copolymer composition in blends of LCPU-M and PS-*co*-VPh measured at 180 °C for different blend compositions.

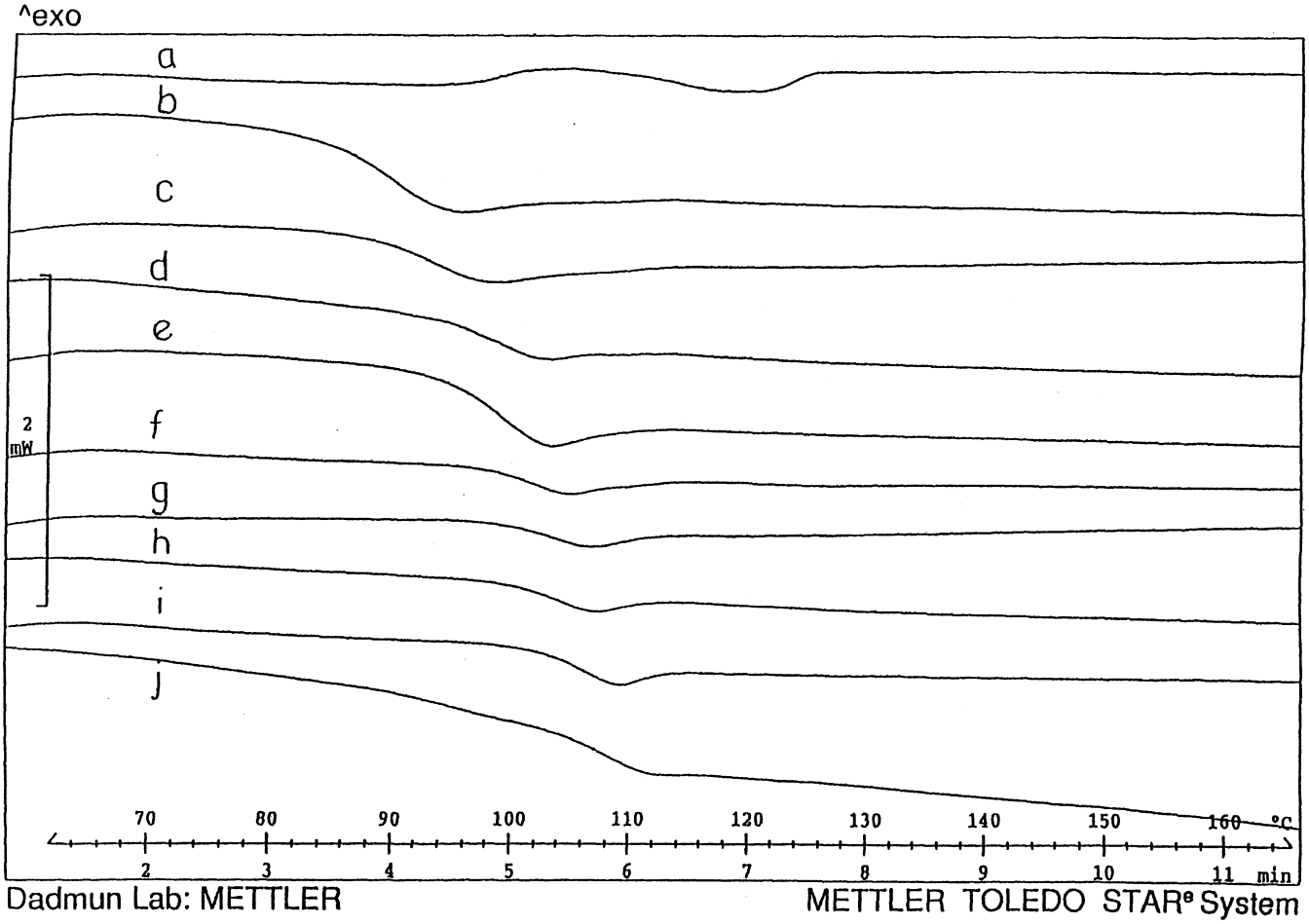

Figure 8. Representative DSC curves of blends containing LCPU-M and PS-*co*-VPh(30). Compositions of the blends are (LCPU/PS-*co*-VPh(30) wt/wt) (a) 45/55, (b) 40/60, (c) 35/65, (d) 30/70, (e) 25/75, (f) 20/80, (g) 15/85, (h) 10/90, (i) 5/95, and (j) 0/100.

for the PS-*co*-VPh(5) blend and increases to 40% LCP for the PS-*co*-VPh(40) blend and then decreases back to 15% LCP for the PS-*co*-VPh(50) blend. This agreement between theoretical and experimental data suggests miscibility in these blends at low LCP content. Moreover, the change in the critical LCP concentration described above correlates well to the intermolecular hydrogen-bonding information attained by FTIR, where

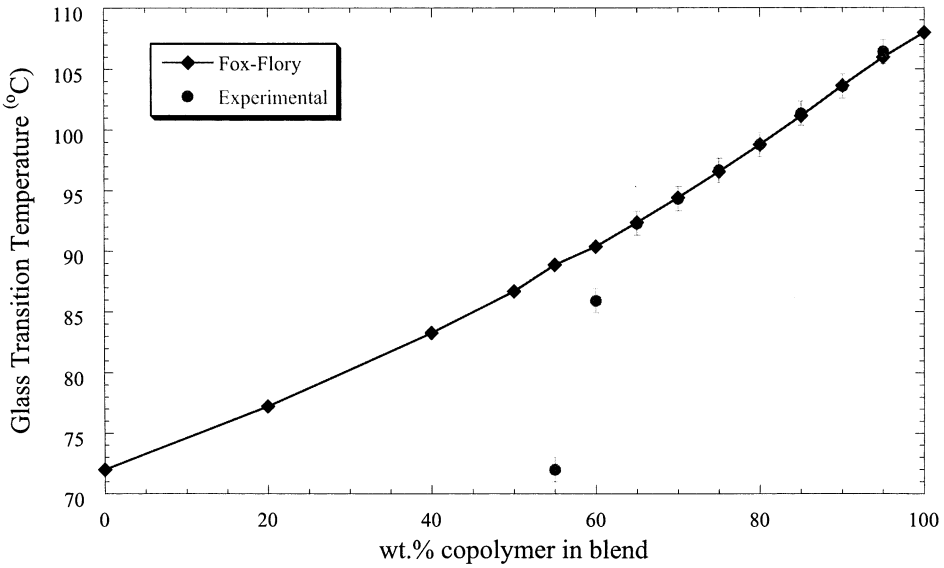

Figure 9. Experimental and theoretical glass transition temperatures of blends containing PS-*co*-VPh(30) and LCPU-M.

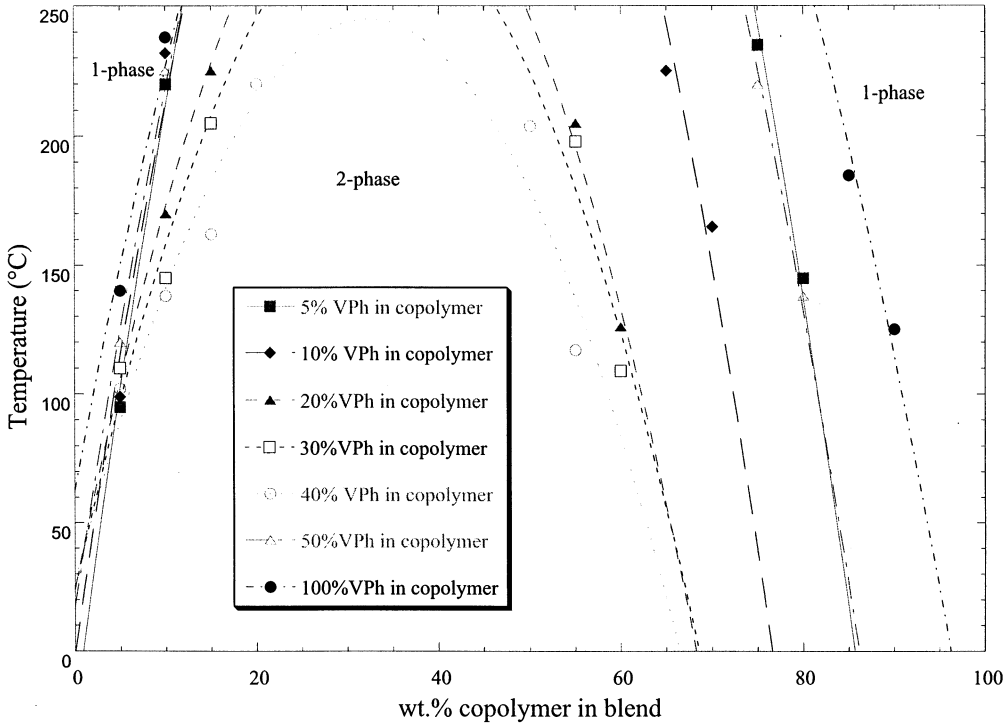

Figure 10. Phase diagram of blends containing LCPU-M and PS-*co*-VPh as determined from phase contrast optical microscopy. Note that the lines are merely fits to a parabola and are meant to guide the eye, not to denote exact phase boundaries.

the blend with the optimum extent of intermolecular hydrogen-bonding appears to have the largest miscibility window.

To more fully understand the phase behavior of these blends, optical microscopy was used to map out their phase diagrams as temperature−composition plots. These plots for the blends of LCPU-M with PS-*co*-VPh are shown in Figure 10. Inspection of this figure shows that as the composition of the amorphous copolymer increases from 10% to 40% vinylphenol, the miscibility window steadily increases. However, as the composition of the copolymer is further increased to 50% and 100%, the miscibility window becomes smaller. This is a very similar trend to what was observed for the LCPU/PS-*co*-VPh blends, where the miscibility window began to decrease above 20% VPh in the copolymer (Figure 3).

Discussion

In the Introduction, it was argued that, by optimizing the extent of intermolecular interactions, the enthalpy of mixing the LCP and an amorphous polymer would become conducive to form a miscible blend. Mathematically, this can be seen by examining the thermodynamic formula, $\Delta G = \Delta H - T\Delta S$, where ΔG is the change in the free energy of the system as it is mixed, ΔH is the change in the enthalpy for the same process, and ΔS is its entropy change. The miscible system is stable if ΔG of this process is negative. However, as is known from Flory−Huggins theory, ΔS is very small for mixing two long-chain molecules, and therefore a modestly positive ΔH of mixing will result in a phase-separated system. By introducing significant hydrogen-bonding, it is hoped

that ΔH will become sufficiently small (or negative) to allow the formation of a miscible system. This argument assumes that formation of the intermolecular hydrogen bonds does not significantly lower the entropy of mixing, an assumption that may or may not be correct. However, inspection of the FTIR and phase behavior data of the system presented in this paper and in our previously examined system[36] provides some insight into the feasibility of using this scheme to induce miscibility in other blends containing a liquid crystalline polymer.

The dependence of ΔH, ΔS, and thus ΔG on the extent of intermolecular hydrogen-bonding can be accounted for by denoting the change in free energy of mixing a blend that can undergo intermolecular hydrogen-bonding by

$$\Delta G = \Delta H - T\Delta S = \Delta H_{FH} + \Delta H_{HB} - T\Delta S_{FH} - T\Delta S_{HB}$$

where ΔH_{FH} is the Flory−Huggins enthalpy that accounts for the dispersion interactions between the molecules, $\Phi_A\Phi_B\chi$, ΔS_{FH} is the Flory−Huggins combinatorial entropy of mixing, ΔH_{HB} is the change in the enthalpy of mixing due to the formation of intermolecular hydrogen bonds, and ΔS_{HB} is the change in the entropy of mixing due to the formation of intermolecular hydrogen bonds. Moreover, increasing the amount of intermolecular interactions lowers ΔH_{HB} and ΔS_{HB}. The variation in hydrogen-bonding, however, is brought about by altering the composition of the amorphous copolymer, and the impact of this change on the enthalpy of the mixing, ΔH_{FH}, must be accounted for. If the χ for LCPU-M and PS is smaller than χ of LCPU-M and poly(vinylphenol), then the addition of the more polar hydroxyl groups to the copolymer will increase the ΔH_{FH} and decrease the propensity to form a miscible system. Of course, if the χ for LCPU-M and PS is larger than χ of LCPU-M and poly(vinylphenol), the opposite trend is expected. While χ for these polymer pairs is not known experimentally, they can be estimated using its relationship to solubility parameters, δ

$$\chi_{AB} = V_r/RT(\delta_A - \delta_B)^2$$

where δ_A is the solubility parameter of component A and δ_B is the solubility parameter of component B. Moreover, the solubility parameters of the polymers can be estimated from group contribution methods.[44] This method gives $\delta_{PS} = 9.5$ (cal cm^{-3})$^{0.5}$, $\delta_{PVPh} = 11.0$ (cal cm^{-3})$^{0.5}$, and $\delta_{LCPU-M} = 9.94$ (cal cm^{-3})$^{0.5}$. Thus

$$\chi_{styrene-LCPU-M} \sim V_r/RT(9.5 - 9.94)^2 \sim 0.1936V_r/RT$$

$$\chi_{VPh-LCPU-M} \sim V_r/RT(11.0 - 9.94)^2 \sim 1.12V_r/RT$$

Therefore, these calculations suggest that addition of hydroxyl groups to the styrenic copolymer *decreases* the miscibility of the copolymer with LCPU-M in the absence of intermolecular hydrogen-bonding.

Correlation of this concept to the system studied here is enlightening—in particular, examination of the 80 wt % curve in Figure 6 and relating it to the phase behavior shown in Figure 10. It is important to note that all curves shown in Figure 6 are taken at 180 °C, well above the nematic-to-isotropic transition of the LCPU; there is no orientational component to the free energy of mixing.[50] This curve in Figure 6 can be separated into two parts: the low concentration of −OH in the copolymer (ca. <40%), where the percent of intermolecular hydrogen bonds increases with increasing amount of −OH, and the high concentration of −OH in the copolymer (ca. >40%), where the percent of intermolecular hydrogen bonds remains relatively constant. For this curve, the ΔS_{FH} contribution to the ΔG can be approximated as constant as each point corresponds to blends with constant composition and similar molecular weights. Therefore, any changes in the phase diagram with copolymer composition must be due to changes in ΔH_{FH}, ΔH_{HB}, or ΔS_{HB}.

Below 40% vinylphenol in the copolymer, the extent of intermolecular hydrogen-bonding increases with increasing vinylphenol content. As mentioned above, increasing the amount of intermolecular hydrogen bonds lowers the ΔH_{HB} enthalpic contribution to the free energy of mixing favoring miscibility, but the entropic contribution, ΔS_{HB}, decreases and ΔH_{FH} increases, both favoring phase separation. However, inspection of Figure 10 shows that the miscibility window increases in this regime (−OH < 40%), demonstrating that the increase in hydrogen-bonding and its direct contribution to the enthalpy dominates the phase behavior of the blend at low −OH concentration. Above 40% vinylphenol in the copolymer, however, shows a leveling off of the amount of intermolecular hydrogen bonds, which translates to no change in ΔH_{HB} or ΔS_{HB}. Thus, the phase behavior is dominated by ΔH_{FH} in this regime where the increasing hydroxyl content of the styrenic copolymer increases the drive to phase separate, decreasing the miscibility window. Similar discussion and correlations between the phase behavior data and FTIR data for the LCPU/P(S-*co*-VPh) blend[36,45] lead to similar conclusions and guidelines.

This discussion concentrates on the blends that contain 80% amorphous copolymer as they are miscible at all copolymer compositions at 180 °C. It is interesting, however, that each of the curves in Figure 6 shows the same trends regardless of copolymer composition, even though some of these blends are immiscible. This is surprising as previous theories[5,51,52] to understand and utilize hydrogen-bonding in the production of miscible blends have counted the number of hydrogen-bonded species and compared them to the amount of hydrogen bonds in a miscible blend. While the systems studied here can be understood using these theories,[53,54] the data in this paper offer an additional method to interpret and utilize intermolecular hydrogen-bonding between polymers to induce miscibility.

Thus, these experiments provide guidelines by which the optimization of intermolecular hydrogen-bonding can be utilized to induce miscibility in a blend. Inclusion of functional groups in a polymer chain that can form specific interactions with another polymer improves the enthalpy of mixing these two polymers. Our results show that the optimal amount of intermolecular interactions occurs when these functional groups are spaced out along the polymer chain. Moreover, if the inclusion of these functional groups into the chain *increases* the dispersion forces between the two polymers, as denoted by the traditional Flory−Huggins χ parameter excluding the specific interactions, the system that provides the optimal extent of intermolecular interactions should provide the broadest miscibility window in the blend phase diagram. Conversely, if the inclusion of the functional groups in the polymer decreases the disper-

sion forces (i.e., χ), the system with the broadest miscibility window should be the system where every monomer is functionalized.

Conclusion

The results described in this paper demonstrate, not surprisingly, that the elimination of intramolecular hydrogen-bonding in a liquid crystalline polyurethane increases the amount of intermolecular hydrogen-bonding that the LCPU can form with another polymer. Additionally, the results also demonstrate that spacing the functional groups that participate in this hydrogen-bonding on the other polymer dramatically impacts the amount of hydrogen-bonding, in agreement with other studies. The spacing of functional groups that shows the optimal extent of intermolecular hydrogen-bonding also corresponds to the blend with the broadest miscibility.

Acknowledgment. The authors thank the National Science Foundation, Division of Materials Research, for financial support (CAREER-DMR-9702313) which funded this research.

References and Notes

(1) Solc, K. *Polymer Compatibility and Incompatibility: Principle and Practices*; MMI Symp. Ser. Vol. 3; Harwood: Cooper Station, NY, 1981.
(2) Patterson, D. *Polym. Eng. Sci.* **1982**, *22*, 64.
(3) Walsh, D. J.; Huggins, J. S.; Maconnachie, A. *Polymer Blends and Mixtures*; Martinus Nijhoff Publishers: Dordrecht, 1985; Vol. 1.
(4) Rudolph, H. *Polym. J.* **1985**, *17*, 13.
(5) Coleman, M. M.; Graf, J. F.; Painter, P. C. *Specific Interactions and the Miscibility of Polymer Blends*; Technomic Publishing Co.: Lancaster, PA, 1991.
(6) Coleman, M. M.; Painter, P. C. *Prog. Polym. Sci.* **1995**, *20*, 1.
(7) Rudolph, H. *Makromol. Chem. Macromol. Symp.* **1988**, *16*, 57.
(8) Landry, M. R.; Massa, D. J.; Landry, C. J. T.; Teegarden, D. M.; Colby, R. H.; Long, T. E.; Henrichs, P. M. *J. Appl. Polym. Sci.* **1994**, *54*, 991.
(9) Kwei, T. K.; Pearce, E. M.; Ren, F.; Chen, J. P. *J. Polym. Sci., Part B: Polym. Phys.* **1986**, *24*, 1597.
(10) Zhu, K. J.; Chen, S. F.; Ho, T.; Pearce, E. M.; Kwei, T. K. *Macromolecules* **1990**, *23*, 150.
(11) Wissburn, K. F. *J. Rheol. (N.Y.)* **1981**, *25*, 619.
(12) Wissburn, K. F.; Griffin, A. C. *J. Polym. Sci., Polym. Phys. Ed.* **1982**, *20*, 1835.
(13) Wissburn, K. F. *Br. Polym. J.* **1980**, *12*, 163.
(14) Cogswell, F. N. *Br. Polym. J.* **1980**, *12*, 170.
(15) Prasadarao, M.; Pearce, E. M.; Han, C. N. *J. Appl. Polym. Sci.* **1982**, *27*, 1343.
(16) Takayanagi, M.; Ogata, T.; Morikawa, M.; Kai, T. *J. Macromol. Sci., Phys.* **1980**, *B17*, 591. Hwang, W. F.; Wiff, D. R.; Verschoore, C.; Price, G. E.; Helminiak, T. E.; Adams, W. W. *Polym. Eng. Sci.* **1983**, *23*, 784. Hwang, W. F.; Wiff, D. F.; Benner, C.; Helminiak, T. E. *J. Macromol. Sci., Phys.* 1983, *B22*, 231.
(17) Pawlikowski, G. T.; Dutta, D.; Weiss, R. A. *Annu. Rev. Mater. Sci.* **1991**, *21*, 159.
(18) Painter, P. C.; Tang, W. L.; Graf, J. F.; Thomson, B.; Coleman, M. M. *Macromolecules* **1991**, *24*, 3929.
(19) Stein, R. S.; Sethumadhavan, M.; Gaudhania, R. A.; Adams, T.; Guarrera, D.; Roy, S. K. *Pure Appl. Chem.* **1992**, *29*, 517. Cowie, J. M. G.; Nakata, S.; Adams, G. W. *Macromol. Symp.* **1996**, *112*, 207.
(20) Dadmun, M. D.; Han, C. C. *Mater. Res. Soc. Symp. Proc.* **1993**, *305*, 171.
(21) Tsou, L.; Sauer, J. A.; Hara, M. *Polymer* **2000**, *41*, 8103.
(22) Weiss, R. A.; Ghebremeskel, Y.; Charbonneau, L. *Polymer* **2000**, *41*, 3471.
(23) Flory, P. J. *Principles of Polymer Chemistry*; Cornell University Press: Ithaca, NY, 1953.
(24) Flory, P. J. *J. Chem. Phys.* **1942**, *10*, 51.
(25) Huggins, M. L. *J. Am. Chem. Soc.* **1942**, *64*, 1712.
(26) Flory, P. J. *Macromolecules* **1978**, *11*, 1138.
(27) Flory, P. J. *J. Am. Chem. Soc.* **1965**, *87*, 1833.
(28) Painter, P. C.; Graf, J. F.; Coleman, M. M. *J. Chem. Phys.* **1990**, *10*, 6166.
(29) Vetysmann, B. A.; Painter, P. C. *J. Chem. Phys.* **1993**, *99*, 9272.
(30) Coleman, M. M.; Pehlert, G. J.; Painter, P. C. *Macromolecules* **1996**, *29*, 6820.
(31) Pehlert, G. H.; Painter, P. C.; Veytsman, B.; Coleman, M. M. *Macromolecules* **1997**, *30*, 3671.
(32) Hu, Y.; Painter, P. C.; Coleman, M. M. *Macromolecules* **1998**, *31*, 3394.
(33) Pehlert, G. H.; Painter, P. C.; Coleman, M. M. *Macromolecules* **1998**, *31*, 8423.
(34) Radmard, B.; Dadmun, M. D. *Polymer* **2001**, *42*, 1591.
(35) Painter, P. C.; Veytsman, B.; Kumar, S.; Shenoy, S.; Graf, J. F.; Xu, Y.; Coleman, M. M. *Macromolecules* **1997**, *30*, 932.
(36) Painter, P. C.; Berg, L. P.; Veytsman, B.; Coleman, M. M. *Macromolecules* **1997**, *30*, 7529.
(37) Pruthtikul, R.; Painter, P. C.; Coleman, M. M.; Tan, N. R. *Macromolecules* **2001**, *34*, 4145.
(38) Viswanathan, S.; Dadmun, M. D. *Macromol. Rapid Commun.* **2001**, *22*, 779.
(39) Viswanathan, S.; Dadmun, M. D. *Macromolecules* **2002**, *35*, 5049−5060.
(40) Tang, W. L.; Coleman, M. M.; Painter, P. C. *Macromol. Symp.* **1994**, *84*, 315.
(41) Khatri, C. A.; Vaidya, M. M.; Levon, K.; Jha, S. K.; Green, M. M. *Macromolecules* **1995**, *28*, 4719.
(42) Teegarden, D. M.; Landry, C. J. T. *J. Polym. Sci., Part B: Polym. Phys.* **1995**, *33*, 1933.
(43) Landry, C. J. T.; Massa, D. J.; Teegarden, D. M.; Landry, M. R.; Henrichs, P. M.; Colby, R. H.; Long, T. E. *Macromolecules* **1993**, *26*, 6299.
(44) Stenhouse, P. J.; Valles, E. M.; Kantor, S. W.; MacKnight, W. J. *Macromolecules* **1989**, *22*, 1467.
(45) Mihara, T.; Naoyuki, K. *Polym. J.* **1997**, *29*, 138.
(46) Ledwidth, A.; Rahnema, M.; Sengupta, P. K. *J. Polym. Sci., Polym. Chem. Ed.* **1980**, *8*, 2239.
(47) Coleman, M. M.; Lee, K. H.; Skrovanek, D. J.; Painter, P. C. *Macromolecules* **1986**, *19*, 2149.
(48) Dean, L.; Brisson, J. *Polymer* **1998**, *39*, 793.
(49) Lee, J. Y.; Painter, P. C.; Coleman, M. M. *Macromolecules* **1988**, *21*, 346.
(50) Flory, P. J.; Ronca, G. *Mol. Cryst. Liq. Cryst.* **1979**, *54*, 289.
(51) Veytsman, B. A. *J. Phys. Chem.* **1990**, *94*, 8499.
(52) Panayiotou, C.; Sanchez, I. C. *J. Phys. Chem.* **1991**, *95*, 10090.
(53) Viswanathan, S. PhD Disseration, University of Tennessee, 2002.
(54) Viswanathan, S.; Dadmun, M. D. Submitted for publication.

MA021520C